Aquaculture 566 (2023) 739162

Contents lists available at ScienceDirect

Aquaculture

journal homepage: www.elsevier.com/locate/aquaculture

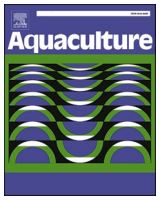

Lumpfish *Cyclopterus lumpus* reproduction: Pituitary gene expression, physiological and morphological changes accompanying gonadal maturation

Eva Andersson [a,1], Elsa Denker [b,1], Birgitta Norberg [c], Rüdiger W. Schulz [a,d], Sara Olausson [c], Anders Thorsen [a], Sigurd O. Stefansson [b], Albert K.D. Imsland [b,e,*]

[a] Institute of Marine Research, Postbox 1870 Nordnes, 5817 Bergen, Norway
[b] Department of Biological Sciences, University of Bergen, High Technology Centre, 5020 Bergen, Norway
[c] Institute of Marine Research, Austevoll Research Station, Sauganeset 16, 5392 Storebø, Norway
[d] Utrecht University, Science Faculty, Department Biology, Padualaan 8, NL-3584, CH, Utrecht, the Netherlands
[e] Akvaplan-niva Iceland Office, Akralind 4, 201, Kópavogur, Iceland

ARTICLE INFO

Keywords:
Cyclopterus lumpus
Annual reproductive cycle
GnRH receptor
fshb
lhb
Sex steroids

ABSTRACT

Lumpfish is the most important cleanerfish species in Atlantic salmon farming. Detailed information on the gonadal maturation process is a prerequisite for year-round production of juvenile lumpfish. In the present study we have described physiological, morphological and endocrine events associated with the annual reproductive cycle in lumpfish of both sexes. Female lumpfish matured at a body weight close to 2 kg and were capable of spawning two egg batches, one in February/March and one in May/June. Male lumpfish could be stripped for sperm most of the year. The appearance of spawning males with high 11-KT concentrations and clearly developed secondary sexual characters was synchronized with female spawning. From the onset of maturation to the periovulatory stages in females, pituitary transcript levels of *gnrhr2ba1* and *lhb* increased in a correlated manner, together with an increase in GSI and in circulating E2 concentrations. In contrast, a high individual variation of *fshb* transcript levels was observed, potentially reflecting the bimodal oocyte development with oocytes at different developmental stages present in the ovary at the same time. The onset of pubertal testis growth concurred with an increase in pituitary *fshb* and *lhb* transcript levels, while plasma 11-KT concentrations increased at later stages, correlating with a *gnrhr2ba1* increase. It appears that spermatogenesis and testis growth is regulated by Fsh and can proceed in the presence of low androgen levels.

1. Introduction

The biological control of sea lice in Atlantic salmon farming by use of lumpfish (*Cyclopterus lumpus* L. 1758) and various species of wrasses as cleanerfish has become a feasible alternative due to the increased occurrence of resistant lice, the reduced public acceptance of chemotherapeutic use in food production, and the urgent need for an effective and sustainable method of parasite control in Atlantic salmon aquaculture (Denholm et al., 2002; Boxaspen, 2006; Imsland et al., 2014a–c; Powell et al., 2018; Treasurer, 2018). Wild stocks of lumpfish do not meet the demands of the salmon aquaculture industry and consequently, aquaculture production of this species has increased rapidly, from around 400,000 individuals in 2012 to over 30 million in 2017, according to official statistics (Norwegian Directorate of Fisheries, 2019).

Farmed cleanerfish are preferred due to better biosecurity through vaccination and screening programs, stocking at optimum times and sizes, and allowing to reduce the reliance on wild caught fish. As lumpfish tolerate lower temperatures than wrasses, their implementation was boosted principally in the northern parts of Norway. Initially, production of juveniles was solely based on wild-caught broodstock, where eggs were stripped, incubated, hatched, and juveniles reared to suitable size for transfer to commercial cages. The steady increase in demand of lumpfish has resulted in a gradual move from wild caught breeders towards intensive cultivation, and a breeding program for

* Corresponding author at: Department of Biological Sciences, University of Bergen, High Technology Centre, 5020 Bergen, Norway.
E-mail address: albert.imsland@akvaplan.niva.no (A.K.D. Imsland).
[1] Equal authorship between Andersson and Denker.

https://doi.org/10.1016/j.aquaculture.2022.739162
Received 26 September 2022; Received in revised form 18 November 2022; Accepted 12 December 2022
Available online 21 December 2022

lumpfish was established in 2017.

Lumpfish are widely distributed across a large area on both sides of the North Atlantic Ocean (Vasconcelos et al., 2004; Bañón et al., 2008; Pampoulie et al., 2014; Jónsdóttir et al., 2018). Natural spawning in lumpfish occurs in spring and early summer (March–July, Davenport, 1985; Mitamura et al., 2012; Kennedy et al., 2015; Kennedy, 2018). Spawning of lumpfish often takes place in shallow sub-tidal waters when temperatures reach around 4 °C (Collins, 1976; Daborn and Gregory, 1983). Little is known about the regulation of the reproductive cycle and gametogenesis in lumpfish and the scarce data available is either based on surveys and specimens captured during roe fisheries (Kennedy et al., 2015; Kennedy, 2018; Kennedy and Olafsson, 2019), or on fish maturing in culture under various manipulated photoperiod or temperature regimes (Imsland et al., 2018, 2019; Pountney et al., 2020). The lumpfish is a determinate spawner and ovarian development takes at least 8 months (Kennedy, 2018). Lumpfish females have been observed to spawn a maximum of two egg batches per season with a similar number of eggs in each batch and a relative fecundity of ca 60 eggs·g^{-1}, giving a total fecundity 50,000–220,000 eggs per female (Gauthier et al., 2017; Kennedy, 2018). Reported size of hydrated eggs/oocytes ranges from 1.63 to 1.64 mm in fish caught in the Gulf of St Lawrence (Gauthier et al., 2017) to 2.05–2.50 mm in fish caught off Iceland, the first batch showing larger eggs than the second (Kennedy, 2018).

Teleost fish exhibit different reproductive strategies, reflecting, for example, their diverse spawning habitats and degree of parental care. In temperate regions, reproduction is controlled by environmental factors, such as photoperiod, temperature and feed availability, and spawning is timed in order to ensure optimal offspring survival (Bromage et al., 2001). Successful aquaculture is dependent on a stable supply of viable eggs, and this requires good broodstock management routines. The high demand for a stable supply of lumpfish for parasite control also necessitates year-round, seasonally independent production of juveniles. Photoperiod control of the reproductive process has been successfully applied to broodstock to alter the phase of the annual sexual cycles and hence the spawning time in a range of fish species, including lumpfish (e.g. Taranger et al., 2010; Imsland et al., 2018, 2019). Understanding the basic mechanisms that regulate oogenesis and spermatogenesis and timing of events leading to natural sexual maturation and spawning is necessary for controlled reproduction and year-round supply of juveniles.

Reproduction is controlled via the brain-pituitary-gonad (BPG) axis, which responds to environmental and endogenous stimuli such as changes in photoperiod, temperature, and nutritional status (Trudeau, 2022). Briefly, gonadotropin-releasing hormone (GnRH) is the central stimulatory agent while additional inhibitory (for example dopamine), or stimulatory agents (for example secretogranin) modulate gonadotropin release as well. Pituitary GnRH receptors induce production and secretion of the key regulators of reproduction, the gonadotropins follicle-stimulating hormone (Fsh) and luteinizing hormone (Lh). Gonadotropins are released into the bloodstream and regulate gonadal hormone and germ cell production ((Levavi-Sivan et al., 2010). Further, steroids exert complex feedback effects on the pituitary, depending largely on gender and stage of maturation (Fontaine et al., 2020).

Oocyte development has been classified into discrete categories according to morphological characteristics (Wallace and Selman,1990), or functional phases (Brown-Peterson et al., 2011) oroocyte size determined by particle analysis (Thorsen and Kjesbu, 2001), since we do not have functional information, we used the morphological approaches. A histological description of lumpfish oocyte development was made by Pountney et al. (2020), while to our knowledge, there is no published information on spermatogenesis in lumpfish. The objective of the present study was to use morphological classification of lumpfish gonadal development to elucidate molecular and endocrine events associated with sexual maturation in lumpfish of both sexes, and thereby provide a basic characterization of lumpfish maturation.

2. Material & methods

2.1. Phylogenetic reconstructions and synteny mapping

Predicted protein sequences were retrieved from the recently annotated *C. lumpus* genome accessible in GenBank (ID: 86363). For the purpose of verifying paralogy relationships and attempting to address nomenclature issues within vertebrates, we established a broad dataset of sequences from teleost groups but also non-teleost Actinopterygii (a lineage that separated before the teleost-specific duplication 3R), Sarcopterygii, Chondrichthyes, as well as agnathans and non-vertebrate chordates. All sequence references can be found in Figs. S1 and S3. These sequences were aligned using ClustalW in Seaview, blocks for phylogenetic analysis were selected using GBlocks and phylogenetic reconstruction was performed using PhyML. Robustness was assessed through bootstrap replication (100 replicates). Either the sequences from the lamprey *Petromyzon marinus* or the ascidian *Ciona intestinalis* were used as an outgroup for rooting the trees.

Synteny mapping was performed on a representative subset of this dataset, using the Genomicus platform (Singh and Isambert, 2019), and for the species not included in the database, manually using NCBI GeneBrowser. Ohnologues were annotated using the OHNOLOGUES platform (Nguyen et al., 2019).

2.2. Animal rearing and sampling

Juvenile lumpfish (initially $N = 300$, weight 8–10 g) produced by FjordForsk Sogn, Sogndal, Norway (from wild caught broodstock in the Sognefjord) were reared at the ILAB facility, University of Bergen, Norway from November 2016 under simulated natural photoperiod for Bergen (60°N) in water from 100 m depth with a stable temperature (8.5–9 °C) and salinity (33 ‰).

The fish were reared in a single 3-m diameter (7000 L) fiberglass tank and fed a commercial dry diet throughout, with pellet size adjusted to the increase in fish size. Fish density was kept below 30 kg m^{-3}.

Twelve animals (on average 6 males and 6 females) were sacrificed at each of nine time points during the experiment, between autumn 2017 and summer 2018: 28.09.17 (Time point, TP1), 03.11 (TP2), 12.12 (TP3), 25.01.18 (TP4), 23.02 (TP5), 22.03 (TP6), 04.05 (TP7), 19.06 (TP8) and 02.08 (TP9).

After netting the fish were anesthetized in a sub-lethal dose of 500 mg l^{-1} MS222 and body length and weight were recorded to the nearest cm and gram. Blood was drawn from the heart into a 2 ml heparinised syringe and kept on ice until centrifuged (10 min at 1800 rpm and 4 °C). Plasma was collected and stored at −80 °C until steroid analysis. Pictures were taken of each fish for evaluation of secondary sexual characters and for gross morphology of the gonad. The fish were decapitated, and brain and pituitary were removed and kept in RNAlater for gene expression analyses. Gonads were excised and weighed for gonadosomatic index (GSI) calculated as:

$$\text{GSI} = \text{gonad weight (g) x } 100/\text{total body weight (g)}$$

After weighing, one piece of the gonad was fixed in Bouin's solution (Merck, Germany) for histology. For the females, one additional piece was fixed in buffered formalin and stored at room temperature until analysis of oocyte diameter and size frequency distribution.

2.3. Steroid analysis

Steroids were extracted from blood plasma by a method modified from (Pankhurst and Carragher, 1992). Briefly, plasma samples (100 μL) were mixed with 1 mL ethyl acetate, vortexed for 20 s and centrifuged for 3 min at 1800 rpm and 4 °C. The organic phase was collected by a Pasteur pipette and the hydrophilic phase was extracted once more with 1 mL of ethyl acetate. The extracts were evaporated in a Speed Vac centrifuge (Savant 1000, USA), and dissolved in 1 mL buffer (phosphate

0.1 M pH 7.4, 0.4 M NaCl, 1 mM EDTA) by heating (60 °C for 10 min). Extraction efficiency was determined by addition of a known amount of ^{3}H-labelled steroid to the plasma and was >80% for all steroids. The extracted and dissolved steroids were stored at −20 °C until analysis. Enzyme-linked immunosorbent assays were validated for lumpfish and performed according to (Cuisset et al., 1994). Plasma dilutions from female and male lumpfish were parallel to standard curves for E2 and 11-KT. ED80 and ED20 were 0.01 ng ml^{-1} and 0.2 ng ml^{-1} for 11-KT and 0.004 ng ml^{-1} and 0.4 ng ml^{-1} for E2. Internal standards were prepared from mature female and male Atlantic cod plasma extracted as described above. The accepted interassay coefficient of variation was 10% for all steroids; assays with higher deviation of the internal standard were re-run. The intra-assay coefficient of variation was 6.8% for E2 ($N = 10$) and 5.6% for 11-KT (N = 10). E2 antisera, acetylcholine esterase-labelled tracers and microplates precoated with monoclonal mouse antirabbit IgG were supplied by Cayman Chemicals (USA). Antiserum against 11-KT was a kind gift from Dr. David E. Kime. Standard steroids were purchased from Sigma Aldrich (Sigma reference standards). Cross-reactivities for E2 antisera are described by the manufacturer, while details on cross-reactivity for the 11-KT antibody are given by (Cuisset et al., 1994).

2.4. cDNA synthesis and qPCR

Total RNA was extracted from pituitary tissues in RNA later using the RNeasy mini kit (Qiagen), and cDNA synthesized using SuperScript III reverse transcriptase (Invitrogen) and oligo(dT)18. For qPCR, primers for our genes of interest (*gnrhr2ba1*, *gnrhr1ca*, *gnrhr1cb*, *lhb*, and *fshb*) and reference genes (*ef1-a*, *hprt*, and *gapdh1a)* were designed so that each pair contained one primer at an exon/exon junction (all primers can be found in Table 1). Primer specificity was verified by melting curve analysis and amplicon size by gel electrophoresis, and linear regression was used to determine PCR efficiency based on dilution curves (Table 1). qPCR was performed on 1:20 diluted cDNA in duplicates using SybrGreen (BioRad) in 12,5 µl reactions with 200 nM primers. Reactions were loaded in 96-well plates, with each plate containing a common pool sample to allow inter-plate calibration. Plates were run in a CFX96 real-time PCR detection system (BioRad) with the following program: 2 min denaturation at 95 °C, 38 cycles with 15 s denaturation at 95 °C and 25 s annealing /extension at 60 °C or 62 °C (depending on the target), followed by a melting curve analysis.

Three reference genes (*ef1-a*, *hprt*, and *gapdh1a*) were selected after consulting pituitary-specific literature on a wide range of vertebrates, including mammals (Normann et al., 2016; Wang et al., 2018), birds (Zinzow-Kramer et al., 2014) and different fish species (Hodne et al., 2010; Lorgen et al., 2015; Paullada-Salmerón et al., 2016). The best combination of these three genes was determined using RefFinder (Xie et al., 2012 – includes geNorm (Vandesompele et al., 2002), NormFinder (Andersen et al., 2004), BestKeeper (Pfaffl et al., 2004) and Delta-Ct (Silver et al., 2006) algorithmic analyses) after running gene expression for on a representative subset of the whole dataset (Table S1). It was decided to run an index of both *hprt* and *ef1-a* as a reference for relative quantification for our genes of interests. Relative gene expression was calculated according to Pfaffl's model (Pfaffl et al., 2004).

2.5. Histology

Samples fixed in Bouin's fixative were transferred to ethanol (70%), dehydrated, and embedded in paraffin according to conventional techniques. Histological analysis was carried out using 3 µm sections after haematoxylin-eosin staining. The sections were scanned using a Hamamatsu NanoZoomer S60 Digital slide scanner using a 40× objective (resolution: 4.53 pixels/µm; corresponding to approximately 400× when looking in the occular of a microscope).

In order to create a detailed description of ovarian development, ovary samples were classified in 9 subsequent stages of oocyte development as reviewed by (Wallace and Selman, 1990). Testes samples were categorized in 7 groups based on the most advanced germ cell stage and the distribution within the testicular lobules and within the testes.

2.6. Oocyte diameter and size frequency distribution analysis

Pictures of whole mount oocytes in buffered formaldehyde placed in a petri dish were taken using an Olympus SZX-12 stereomicroscope at 12.5 x and a 5 Mpixel Spot Insight camera (resolution: 0.180 pixels/µm). From the pictures the mean diameter of the oocytes was determined by particle analysis (Thorsen and Kjesbu, 2001) from an average of 186 oocytes from each female (range 25–464, SD = 121). This was performed using the open source image analysis program ImageJ (http://rsb.info.nih.gov/ij) and the ObjectJ plugin (http://simon.bio.uva.nl/objectj) in combination with the Elliptical oocytes project (https://sils.fnwi.uva.nl/bcb/objectj/examples/oocytes/Oocytes.htm). All oocyte diameters reported in this work are as measured in their formaldehyde fixed state.

2.7. Statistics

Basic oocyte size statistics were analyzed using STATA 15 (StataCorp LLC) while other statistics were analyzed by Statistica 10 (StatSoft Inc., USA). Differences in reproductive parameters across sampling months and histological stages were assessed by analysis of variance (one way ANOVA), followed by Student-Newman-Keuls post hoc test in cases of

Table 1
Primers used for qPCR analysis, and their properties.

Gene	Primer	Sequence 5′ to 3′	Exon/exon junction	Amplicon length (bp)	Annealing/elongation temperature (°C)	Amplicon Tm (°C)	%E
fshb	*Forward*	GTGGCCTGACCTACGTCAACCTC	No	112	60	82,5	100,95
	Reverse	TCGCTGATGTAGACCGAGTCCTTG	Yes				
lhb	Forward	TGGCCCGTGGCTCCTGCAGAGGC	Yes	162	62	85,5	100,11
	Reverse	GAACGGTATCTTACTGACGGGGTCCTTGG	Yes				
gnrhr1ca	Forward	TGTGACGCTGTATGTCTTCC	No	106	60	79,5	101,16
	Reverse	GGCAGTGCTCACCATCTTTTCC	Yes				
gnrhr1cb	Forward	GCAGCACCTGAGAGACAAAGCAGG	Yes	114	60	82,5	80,75
	Reverse	GAAGGAAAGCACGATGACCACCGTC	No				
gnrhr2ba1	Forward	TTCCTGCCTGTTCCTGCTTCCTC	No	103	62	79,5	97,44
	Reverse	CATTGGATGGCATGTGGTCC	Yes				
gapdh1a	Forward	CACAGTTTTCCACGAGAGAGACC	Yes	154	62	82	101,39
	Reverse	GCTGGGTGCAGAGATGATGAC	No				
ef1a	Forward	TCCAGCTACCCTCCCCTCGGTCGTTTC	Yes	98	60	84	94,31
	Reverse	CCGGATATTTCCTTGTACTCGACAGCC	No				
hprt	Forward	CGTTGGCTACCGACCCGACTTTG	Yes	141	60	79	94,61
	Reverse	GCCTTGTACTTCTCCTTCCCTGATTC	No				

significant ANOVA. Data were checked for homogeneity of variance by Levene's test and for normal distributions using normal plots. Significance was set at $P < 0.05$.

2.8. Ethics

The study was conducted according to the Animal Welfare Act (LOV-2009-06-19-97). The present trial was approved by the local responsible laboratory animal science specialist under the surveillance of the Norwegian Animal Research Authority (NARA) and registered by the authority by the following registration numbers FOTS 23018.

3. Results

3.1. Identification and detection of reproductive gene transcripts of the pituitary in lumpfish

The lumpfish repertoire for the Gnrh/gonadotrope axis consists in 3 *gnrhs* (1,2,3), 5 *gnrh* receptors, and a single copy of *lhb* and *fshb*, and of *lhcg*- and *fsh*- receptors. The present study is centered on the genes expressed in the pituitary, i.e. the GnRH receptors and gonadotropin β subunits (Fig. 1, details in Fig. S1), and further details on the GnRH ligands and gonadotropin receptors can be found as supplementary data

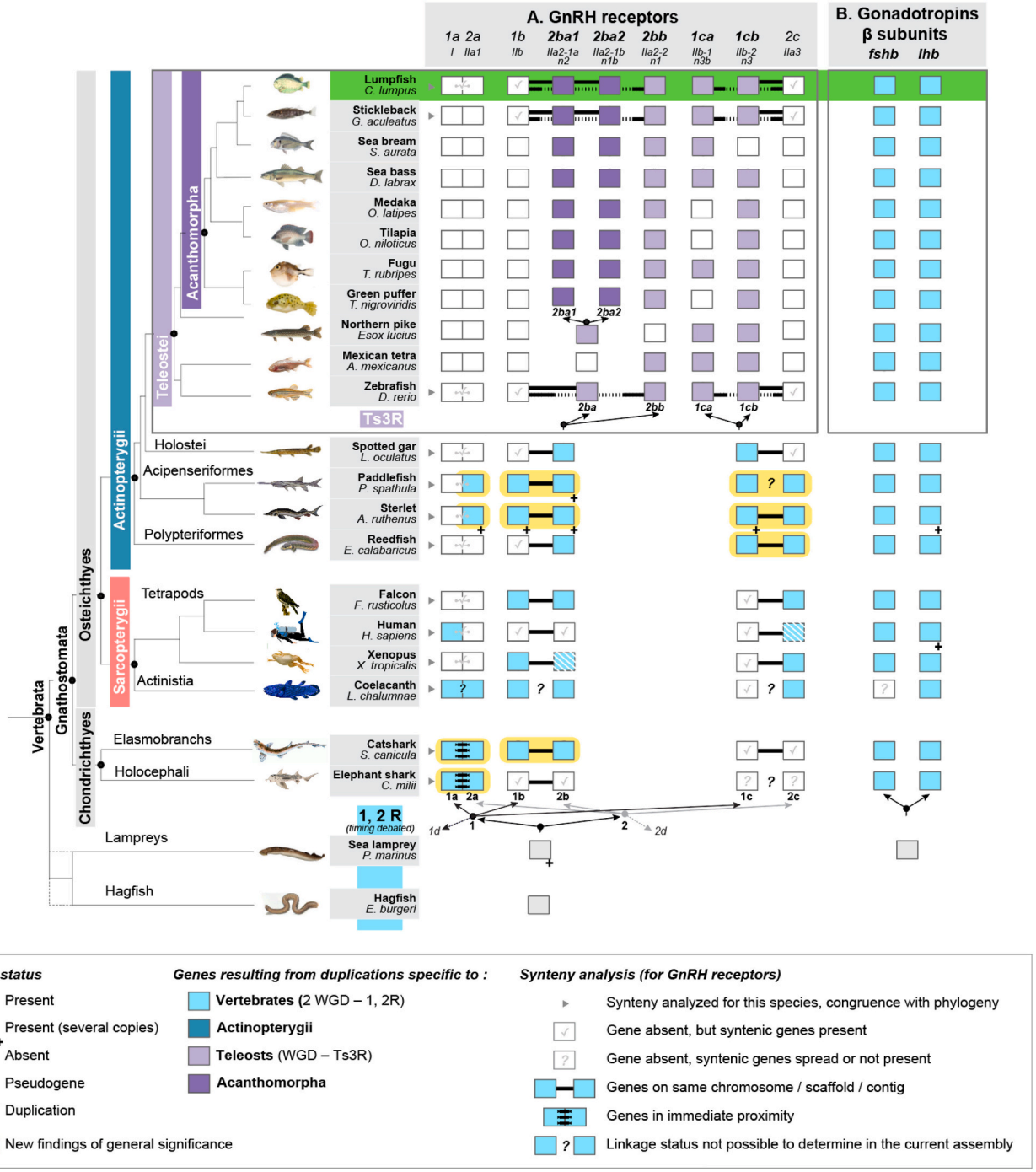

Fig. 1. Lumpfish gene repertoire for the pituitary part of the GnRH-gonadotrope axis. This simplified diagram presents the gene duplications and losses that occurred during vertebrate evolution, alongside the phylogenetic relationship between the presented species. For GnRH receptors, additional syntenic data are presented. All the corresponding phylogenetic and synteny analyses can be found in the supplementary material.

(Fig. S2).

As several nomenclatures have been proposed for Gnrhrs depending on alternative evolutionary scenarios, we deemed it necessary to perform additional investigations, by including previously unstudied groups in our dataset and synteny mapping. Both our phylogenetic (Fig. S1) and synteny (Fig. S3) results were strongly in favor of six vertebrate Gnrhr families, consisting of three sets of genetically linked gene pairs (Fig. 1), we therefore decided to use the nomenclature proposed by Sefideh et al. (2014) and used by Ciani et al. (2020) (*gnrhr*1a/b/c and -2a/b/c) and named the lumpfish genes *gnrhr*2ba1, −2ba2, 2bb, 1-ca and -1cb.

Two out of the five *gnrhr* variants identified in the genome, *gnrhr2bb and gnrhr2ba2,* showed low expression levels (Ct value >34, not shown). *Gnrhr1cb* and *-1ca* had a low relative expression in both sexes throughout the whole experiment (Fig. S4 A-D). *gnrhr1cb* values did not show significant changes between time points (Fig. S4 A-B) and though *gnrhr1ca* presented a statistically significant increase in December in females (Fig. S4C), the relative increase was small, with high individual variation. In contrast, *gnrhr2ba1*, similar to *fshb* and *lhb*, was strongly expressed in both sexes and presented clear signs of regulation between time points (Fig. S4E-J) and, more importantly, between developmental stages (Figs. 7E and 8E). Therefore, we focused our efforts on those three genes for this study.

3.2. Developmental changes along the course of the annual sampling

In females, ovarian growth (calculated as gonadosomatic index, GSI, Fig. 2A) and plasma E2 concentrations (Fig. 2B) increased from January. The GSI increase in females in March is significant compared to September, November, and December (SNK post hoc test, $P < 0.05$, Fig. 2B). These increases were also associated with an increase in individual variation. Both GSI and plasma E2 reached statistically significant peaks in March. The individual distribution showed that GSI and plasma E2 increased in 50% of the females between January and May, an indication that only half of them matured. In addition, there was a relatively high variation between maturing individuals, suggesting heterogeneity in terms of developmental stage.

In males, testes growth varied throughout the year (Fig. 2C). GSI increased in February and May, before decreasing until August. Mean plasma concentrations of 11-KT increased in January and reached a maximum in March and May. This increase was accompanied by a large increase in individual variation. However different from the females, all males except for one individual sampled from January to May showed high GSI levels.

Since this large individual variation in the timing of maturation could mask developmental changes and translate into significant noise in the maturational parameters measured (Fig. S5E-F), we decided to classify the fish not by sampling time but according to the most advanced germ cell stage by using histological analysis.

3.3. Histological analysis of gonadal development

3.3.1. Females

3.3.1.1. Stages. At stage I (Fig. 3A, I) the most advanced oocyte stage was the perinucleolar (Pn) oocyte (Fig. 3A, I inset), in which the nucleoli of the oocyte nucleus were clearly visible. Oocyte diameter ranged from 378 to 487 μm (Fig. 3B, I). Atresia was present in 85% of the individuals at this stage. At stage II, cortical alveoli (Ca) and lipid droplets appeared in the periphery of the cytoplasm (Fig. 3A, II inset) and the oocyte

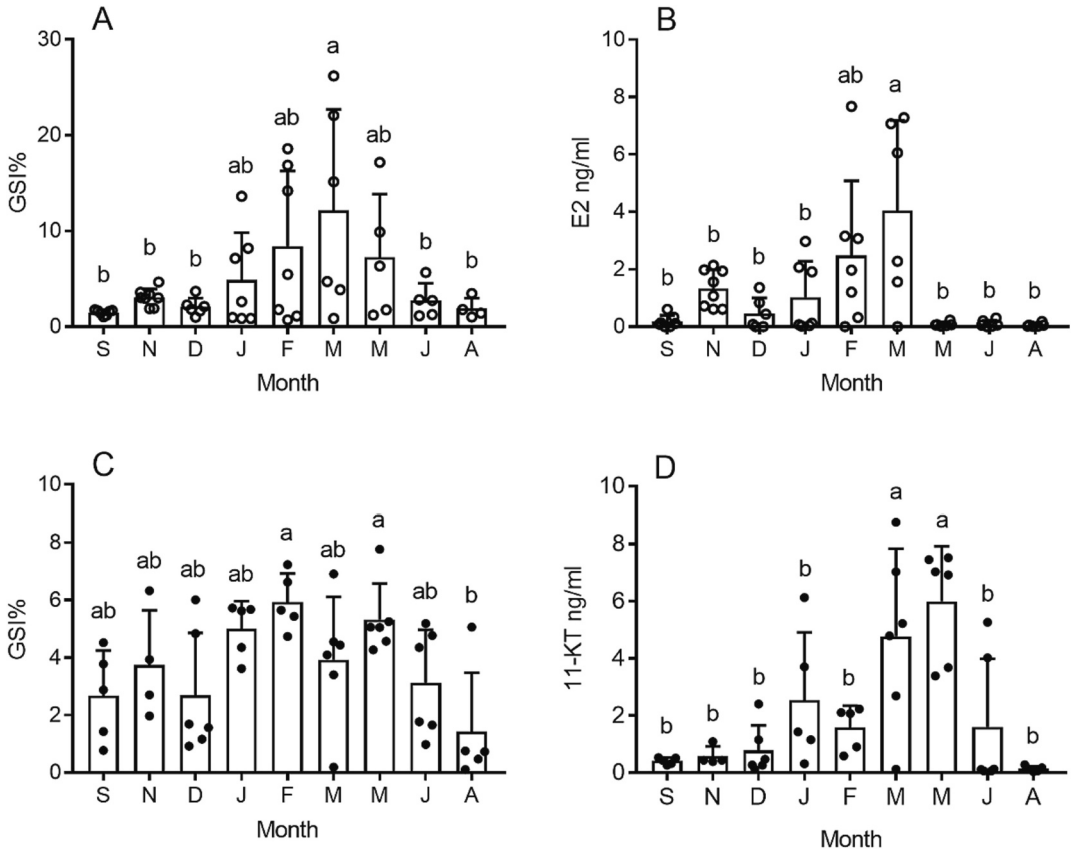

Fig. 2. Gonadosomatic index (GSI) and plasma steroids in lumpfish at nine sampling occasions during one reproductive yearly cycle. (A) GSI (B) plasma 17b-estradiol in females. (C) GSI and (D) plasma 11kT in males. Data are presented both as individual values and as mean and SD. Letters indicate significant differences (Student-Newman-Keuls post hoc test, $P < 0.05$) with "b" as the lowest value, and "a" as the highest value.

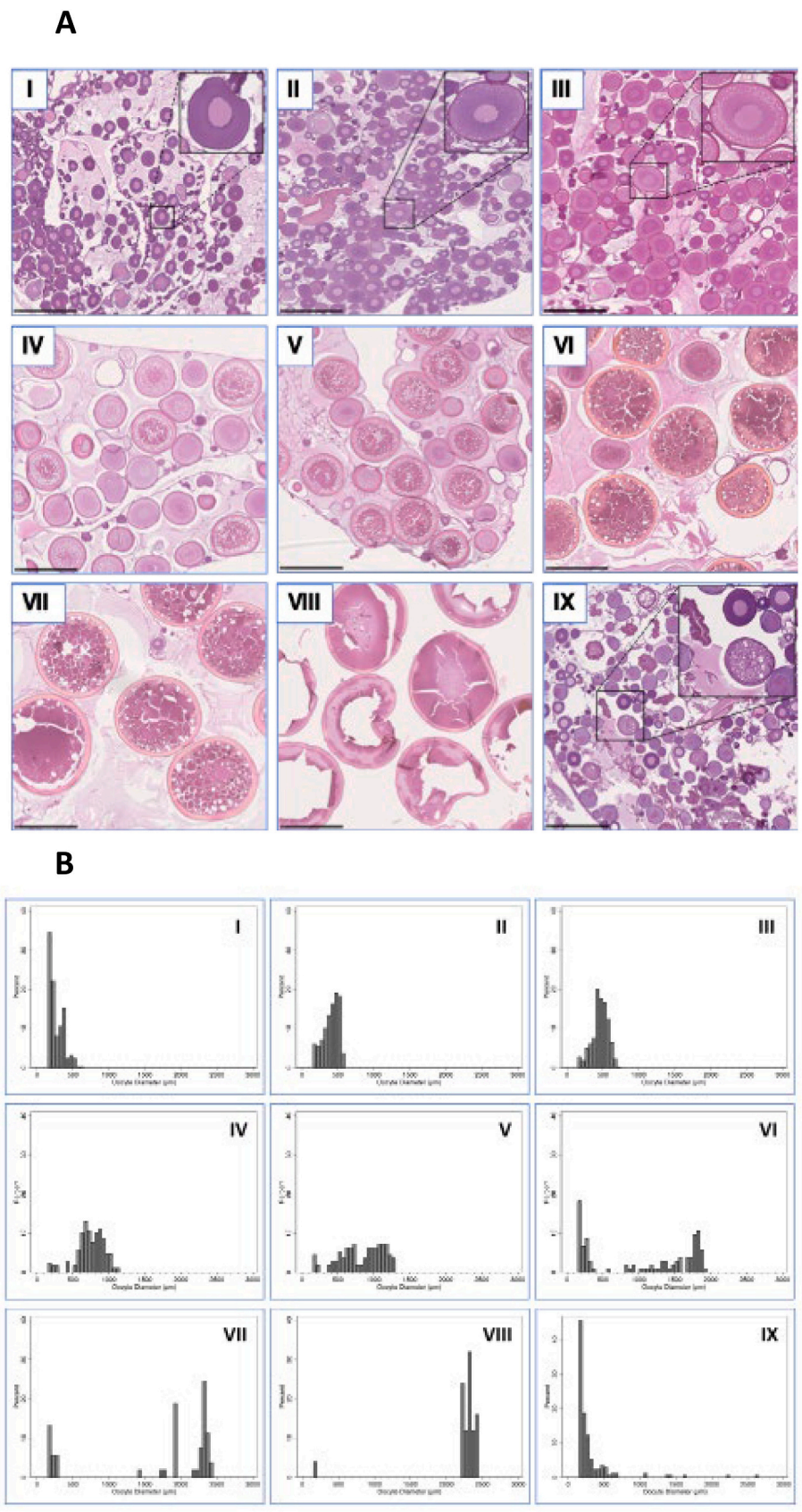

Fig. 3. Representative histological characteristics of the ovary developmental stages. A. Representative photographs of histological sections of lumpfish ovaries. Stage I: Perinucleolus (Pn), II: cortical alveoli, III: early vitellogencic, IV: mid vitellogenic, V: late vitellogenic, VI: early hydrating, VII: mid hydrating, VIII: late hydrating/periovulatory, and IX: postovulatory stage. Insets in I-III shows larger magnification of leading cohort. Inset in IX indicates the presence of post ovulatory follicles and atretic vitellogenic oocytes. Bars indicate 1 mm in all panels. B. Oocyte size-frequency distribution histograms representative of stage I-IX of ovarian development in lumpfish.

diameter range was 480–667 μm (Fig. 3B, II). Large blood vessels were prominent, and atresia was present in 80% of the animals.

At stage III (early vitellogenic stage) yolk accumulation had started (Fig. 3A, III inset). Oocyte diameter range increased to 582–844 μm (Fig. 3B, III). Atretic oocytes were present in 50% of the females in this group.

At stages IV (mid vitellogenic) and V (late vitellogenic), the density of yolk globules increased (Fig. 3A, IV, V) as did the size of the oocytes, ranging from 894 to 1271 μm (stage IV) to 1240–1418 μm in stage V (Fig. 3A and B, IV, V). Further, at stage V, oocytes at earlier stages of vitellogenesis were also present (Fig. 3A and B, IV, V). This became even more evident at stage VI, where the leading cohort (defined statistically as the p95) had further increased in size (1851–1858 μm, Fig. 3A and B, VI) while the second group of oocytes were vitellogenic oocytes at stage IV (Fig. 3A and B, VI). At the first hydration stages VI - VII, the yolk globules were becoming increasingly hydrated and fused into larger, cohesive structures (Fig. 3A, VI, VII). At stage VII, the oocyte diameter range of the leading cohort was 1916–2395 μm (Fig. 3A and B, VII), while the second maturing group was mainly stage VI oocytes (Fig. 3A and B, VII). Atresia was present in 33% of the animals at stages IV-VII. Stage VIII contained late hydrating oocytes with a homogenous appearance (Fig. 3A, VII) and/or ovulated eggs free in the ovarian lumen, at a diameter of 2406–2498 μm (Fig. 3A and B, VII). The post-ovulatory ovaries, stage IX, were identified by the presence of atretic vitellogenic oocytes and postovulatory follicles (POFs) (Fig. 3A, IX inset). Ovaries at this stage contained mainly Pn or Pn and Ca oocytes.

Considering the reproductive phase terminology of Brown-Peterson et al. (2011), our histological stage I relates to the immature phase, our stages II-IV relate to the developing phase (stages II – III: early developing subphase); our stages V-VIII are spawning capable with stages VII – VIII as the actively spawning subphase. Finally, our stage IX is the regressing (cessation of spawning) phase.

3.3.1.2. Oocyte size frequency distribution. The most immature/early developing stages I and II, together with early vitellogenesis (III) formed one single group of oocytes increasing in size (Fig. 3B, I-III). As the leading cohort of oocytes proceeded in vitellogenesis (stage IV and V) it became evident that next to the leading batch, a second, trailing batch was maturing while a portion of the previtellogenic oocytes (Pn, stage I) remained small and was not recruited into maturation (Fig. 3B, IV-V). At stage VII, the leading cohort was close to the maximum oocyte diameter (Fig. 3B, VII) while the second batch had the same size as the most advanced oocytes at stage VI. At stage VIII there was only one single batch of fully mature oocytes together with a portion of small Pn oocytes (Fig. 3B, VIII), suggesting the first batch had been spawned and the second batch had reached maximal size. This difference between stages VII and VIII was systematically observed in all examined individuals (Fig. 4). In stage IX, only Pn oocytes were present, suggesting both maturing batches had been released (Fig. 3B, IX).

3.3.2. Males

Macroscopically, immature testes were composed of several greyish, semi-transparent elevations forming thickenings along a central collecting duct (Fig. S5A). These elevations thickened and enlarged to form multiple lobes, the color of which turned into an opaque, ebony white (Fig. S5B). Microscopically, the greyish and semi-transparent lobes contained spermatogonia and spermatocytes, while the color change and opaqueness was associated with the appearance of large numbers of haploid germ cells, i.e., spermatids and spermatozoa.

Histologically, at stage I, (Fig. 5), spermatogenic tubuli showed a high cell density in the periphery, while a lumen started to appear in many tubuli. The germinal epithelium contained Sertoli cells (arrowhead; Sc), while type A spermatogonia (black arrow; SGA) were the furthest developed germ cell type. In central areas of the testis lobes, tubuli were bigger than in the periphery and appeared partially empty (Fig. 5), seemingly devoid of germ cells. However, they did contain Sc with thin cytoplasmic extensions that spanned a network in this germ cell-free space.

At stage II, spermatogenic tubuli in the periphery had increased in size and more numerous, advanced germ cells were present (Fig. 5, II). A lumen was visible in all tubuli. They contained Sc (black arrowhead), SGA (black arrow) and type B spermatogonia (white arrowhead, SGB). In addition, some apoptotic germ cells were visible (#). Tubuli in the central area of the lobe were larger than in the periphery and contained spermatocytes (*; SPC) and the first spermatids (Ω; SPT), in addition to the cells already encountered in the periphery. Some apoptotic cells were visible in central tubuli (#), and there were still some areas devoid of germ cells, through which Sc sent thin cytoplasmic extensions.

At stage III, all stages of spermatogenesis were present, including spermatozoa (ω; SPZ) (Fig. 5, III). A maturational gradient existed between the periphery, with a higher density of earlier stages (SGA) and new cysts, and more central areas with larger tubuli, where few or no SGA were found. Here, the production of new spermatogenic cysts had ceased, and germ cells in the existing cysts continued spermatogenesis. The first cysts had completed development since spermiation started, i.e., after finishing the final differentiation steps known as spermiogenesis, the cysts opened and released mature SPZ into the lumen of the tubule. In the interstitial tissue of the central area, small groups of Leydig cell (Lc) were visible, however, their cytoplasmic area was still not fully developed. Empty areas devoid of germ cells had become less frequent.

At stage IV, germ cells at all developmental stages were present in the

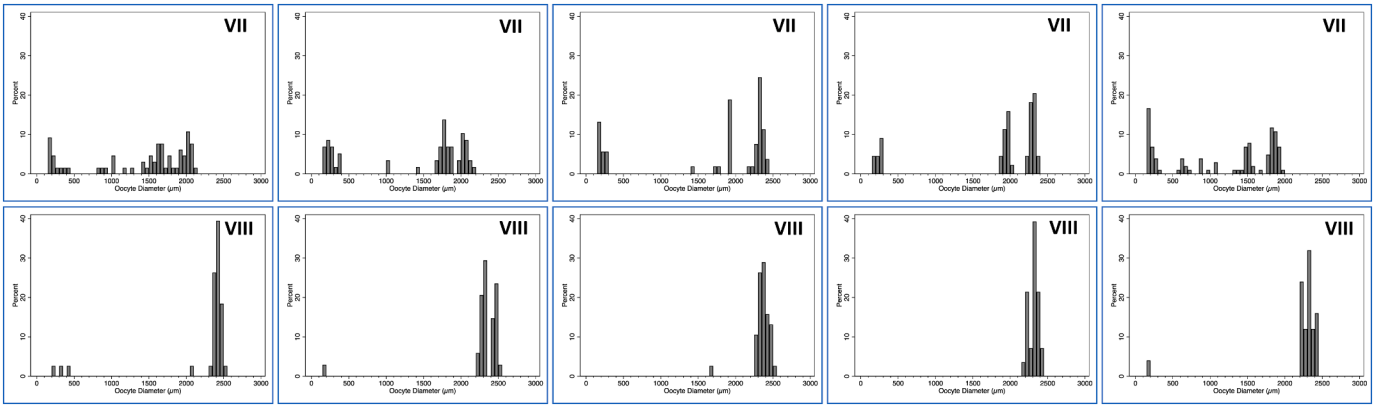

Fig. 4. Detailed oocyte size-frequency distribution histograms for five individuals, comparing stage VII and VIII of lumpfish ovarian development. Lumpfish in stage VII were sampled in February ($N = 2$) and March and VIII in May and June. The number of fish (N) in stage VII was 2 in February and 3 in March, for stage VIII there was 4 in May and 1 in June.

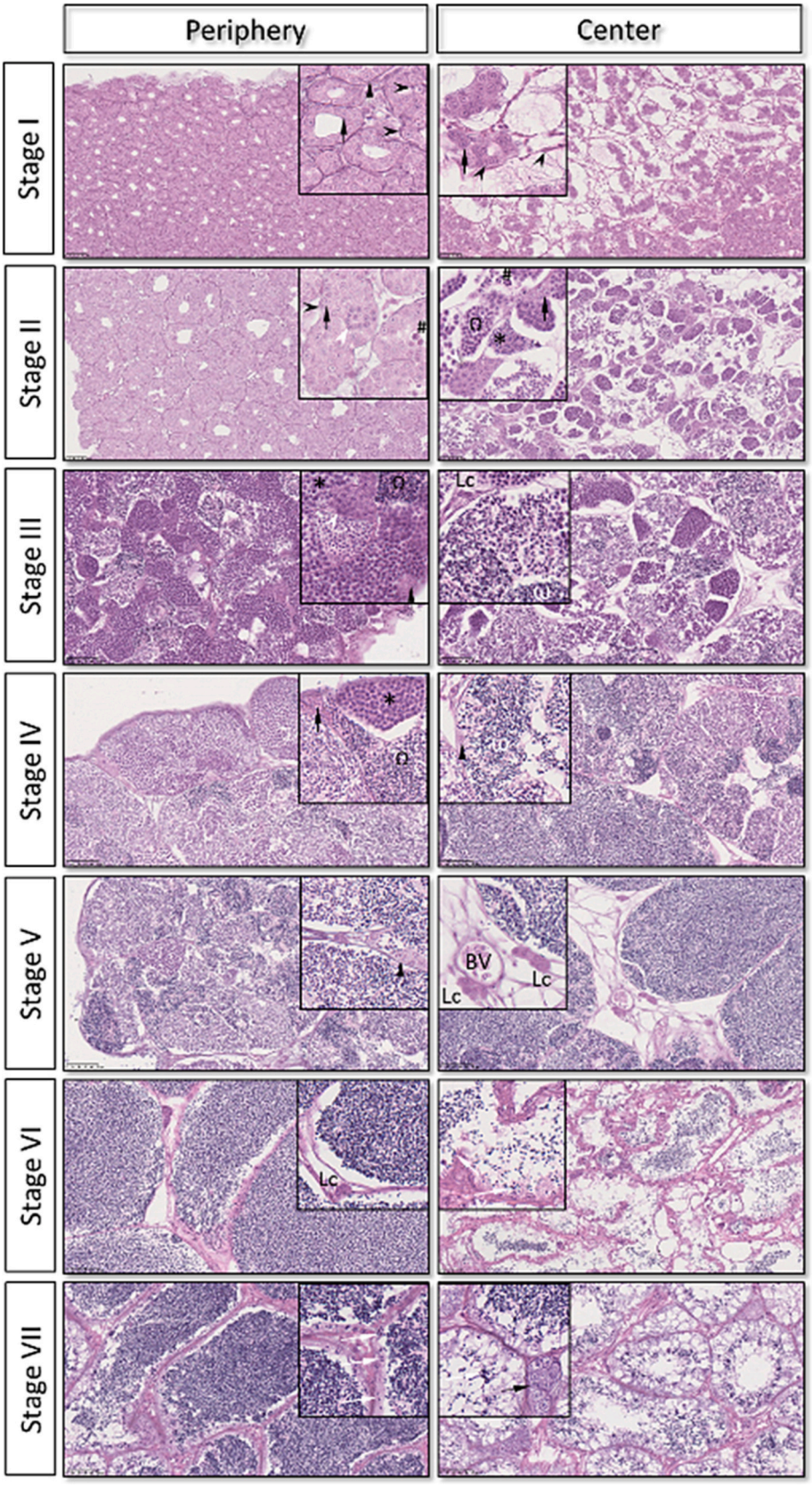

Fig. 5. Histological characteristics of testes development. Representative photographs of histological sections from the peripheral and central areas depicting 7 developmental stages, ranging from immature (Stage I) to the completion of spawning (Stage VII). Black arrowhead, Sertoli cells; arrow, type A spermatogonia; white arrowhead, type B spermatogonia; #, apoptotic germ cells; *, spermatocytes; Ω, spermatids; ω, spermatozoa; Lc, Leydig cells; BV, blood vessels; white arrows, residual spermatozoa being phagocytosed and resorbed by Sertoli cells. Bars indicate 50 μm.

periphery (Fig. 5 IV). However, SGA and SGB were less frequent now also in the periphery, and most cysts had reached the stage of SPC and SPT. The first SPZ appeared in tubular lumina in the periphery. In the center most cysts contained postmeiotic germ cells, i.e., SPT in different phases of spermiogenesis. Moreover, free (spermiated) SPZ were present in many lumina. A few, single SGA associated with Sc were visible in the center (black arrow) but seemed quiescent. Hence, the developmental gradient between periphery and center was still noticeable but has become less steep. Large blood vessels appeared in the center. In the interstitium of the central area, small groups of Leydig cells were present.

In half of the males at stage V, mostly quiescent SGA and mature spermatozoa were present (Fig. 5, V). The other half still showed testes containing a few cysts with SGB, SPC, and some with SPT in the periphery. The gradient between periphery and center remained visible but was reduced as centrally, germ cells had largely completed development. Only a few cysts containing SPT were found completing spermiogenesis, so that free SPZ filled the lumina. Large blood vessels were observed in the center but were also visible in the periphery. In the central area, groups of active Leydig cells were visible. In contrast to the two previous stages, these cells now showed a fully developed cellular/cytoplasmic volume, resulting in a greater distance between nuclei of these cells appearing in small groups in the interstitium.

At stage VI, the only germ cells present were SGA and SPZ (Fig. 5, VI). The gradient between the periphery re-appeared in a different manner. Peripheral tubuli were filled with SPZ and a low number of quiescent SGA. The interstitial area contained Leydig cell groups. In the central area, tubuli were largely empty, residual SPZ were phagocytosed and resorbed by Sertoli cells (white arrows), and SGA had resumed activity and started to repopulate the germinal epithelium in some areas (see stage VII below).

At the final stage VII, SGA and SZ remained the only two cell types present (Fig. 5, VII). However, different from the previous stage, interstitial Leydig cells no longer formed groups, and the individual cells had lost the conspicuous cytoplasmic area. Repopulation with SGA had started in many areas in the center. Next to SGA, the tubuli contained Sc occupied with removing residual spermatozoa. Resorption of SPZ had also started in the peripheral tubuli, where the number of spermatozoa was still quite high, while SGA repopulation was less obvious.

3.4. Annual cycle of gonad maturation

3.4.1. Females

In September all sampled females were at stage II and III. From November to March (except in February) stage IV was also present (Fig. 6A). One female in each of the January to March samplings had oocytes at stage V. Stage VI was present in January and February and VII in February and March, while stage VIII was found in May and June. In June and August, 50% of the sampled females had reached stage IX.

3.4.2. Males

From September to February there was one or two males at stage III, the rest were at stage IV, except in December when also two males at stage II were present (Fig. 6B). In January the first male at stage V was found and this stage was otherwise dominant March and May. Stage VI was first found in May (one individual) and in June in 50% of the animals and in one individual in August. Stage VII was found in 50% of the animals sampled in June, and in one animal in August. The remaining fish in the August sampling were at stage I and II.

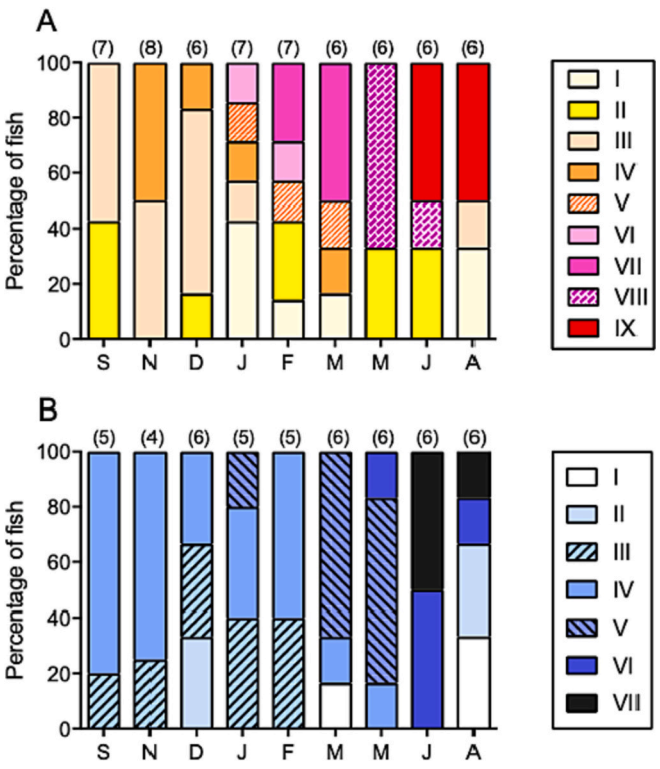

Fig. 6. Gonadal histology in lumpfish ovaries (A) and testes (B) under one reproductive season. The number of animals is indicated on top of the bars.

3.5. Changes in reproductive parameters in relation to histologically determined stages of gonadal development

3.5.1. Females

3.5.1.1. GSI, E2 and pituitary gene expression. GSI was 1–2% in females with oocytes at stages I-III and increased 5-fold at stage IV and V (Fig. 7A). At stage VI-VIII GSIs were significantly higher than at all other stages with a maximum 20-fold higher than in immature females in stage VII. After ovulation GSI levels dropped significantly (stage IX). The variation between individuals was lower when the fish were grouped according to stage rather than by sampling date, reflecting the fact that 2–5 different developmental stages were found at a single time point in females (Fig. 6A).

Plasma E2 concentrations were low in females with oocytes at stage I – III (Fig. 7B), increased 3–4-fold at the mid- and late vitellogenic and early hydration stages IV to VI, followed by a peak at the pre-ovulatory stage VII. Plasma E2 levels were again low in females at ovulation (VIII) and post-ovulation (IX) stages.

Relative changes in pituitary *fshb* mRNA showed large interindividual fluctuations within stages, and no significant changes between stages in females (Fig. 7C).

Transcript levels of *lhb* were low without significant changes in the most immature stages, followed by an increase at stage VI, and reached the highest levels in the late hydration stage VII. *lhb* transcript levels declined at ovulation (stage VIII) to levels similar to stage VI and declined further to low levels in postovulatory stage IX (Fig. 7D).

gnrhr2ba1 transcript levels were low at stage I-III (Fig. 7E), increased significantly in mid- and late vitellogenesis (stages IV-V), and increased further to peak levels at hydration (stages VI and VII). At the ovulatory and postovulatory stages (VIII and IX) the *gnrhr2ba1* transcript levels were again low, similar to the most immature stages I-III.

This data classification approach did not show significant regulation of *gnrhr1cb* and *gnrhr1ca* in female lumpfish (Fig. S6A-B).

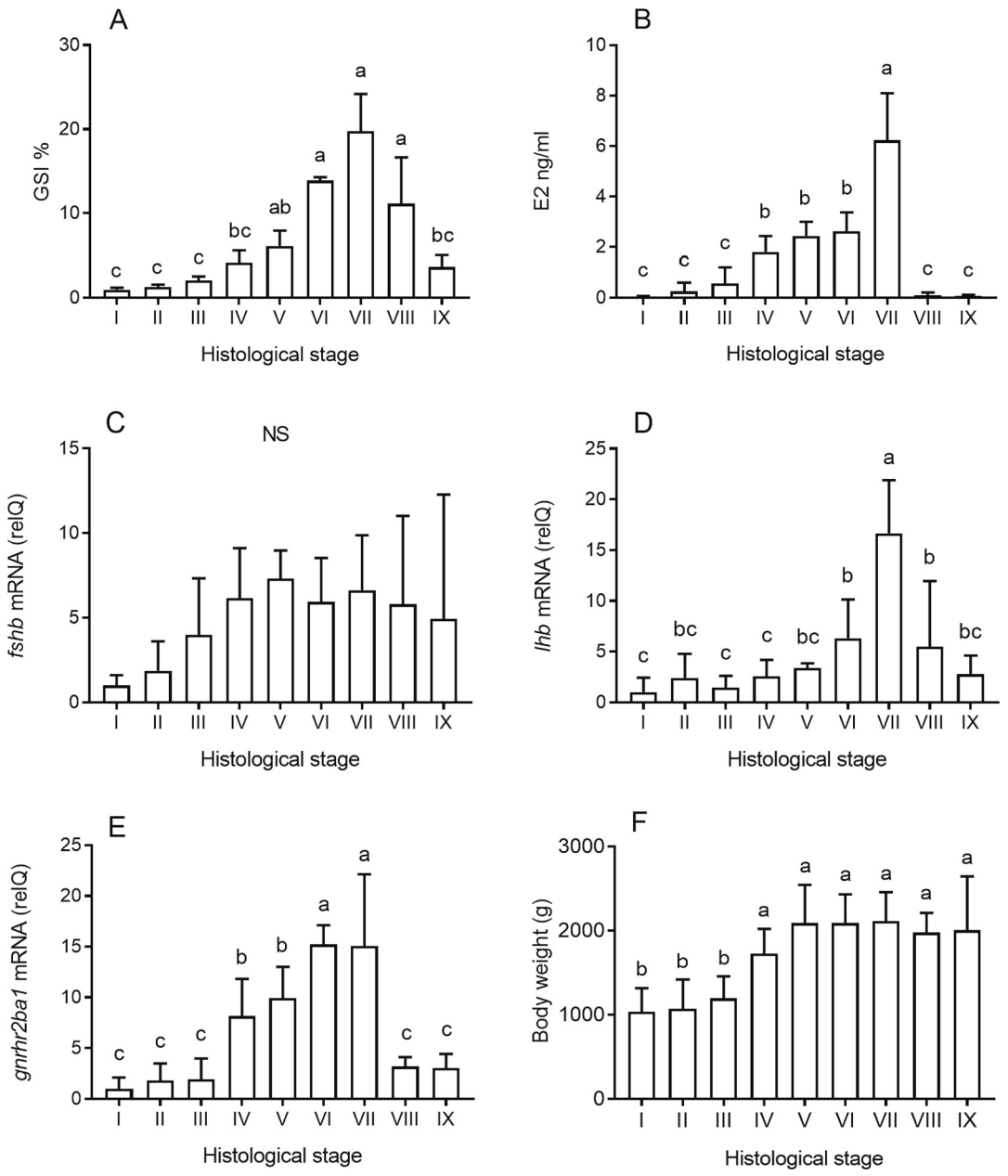

Fig. 7. Comparison of (A) gonadosomatic index (GSI), (B) plasma 17b-estradiol (E2), (C) pituitary *fshb*, (D) *lhb*, (E) *gnrhr2ba1* mRNA levels and (F) body weight in lumpfish females at determined stages of ovarian development. Data are presented as mean and SD. Shared letters indicates statistical similarities. The number of fish (*N*) was 7 in stage I, 10 in stage II, 14 in stage III, 7 in stage IV, 3 in stage V, 2 in stage VI, 5 in stage VII, 3 (5) in stage VIII and 4 (6) in stage IX. Letters indicate significant differences (Student-Newman-Keuls post hoc test, $P < 0.05$) with "a" as the highest value, "b" as the second highest value and "c" as the lowest value.

3.5.2. *Males*

GSI was 0.25 to 1% at stage I and II, increased to a plateau around 4% at stages III-VI and decreased to 1.5% at stage VII (Fig. 8A). Plasma 11-KT concentrations were low or undetectable at the most immature stages (I, II), reached a peak at stage V, decreased at stage VI and decreased further, to low or undetectable levels, at stage VII (Fig. 8B).

Pituitary *fshb* mRNA levels increased 5-fold with the transition from the most immature stages I and II to stage III and IV (Fig. 8C), and reached the highest levels at stage V. At stage VI the levels decreased and at stage VII the levels were as low as at stage I.

Similarly, the transcript levels of *lhb* presented a two-step increase and were highest at stage V. *lhb* transcript levels were low at stage I and II, 2-fold higher at stage III-IV, and increased a further 3-fold to reach a peak at stage V-VI (Fig. 8D) The levels were low in stage VII.

gnrhr2ba1 transcript levels were low at stage I-III, increased gradually to reach the highest levels at stage V, and was again low at VII (Fig. 8E).

This data classification approach did not show significant regulation of *gnrhr1cb* and *gnrhr1ca* in male lumpfish (Fig. S6C-D).

4. Discussion

4.1. *Characterization of the developmental sequence for lumpfish maturation*

In female lumpfish, ovarian weight was low in the most immature stages (histological stages I-III), and there were notable levels of atresia. GSI increased significantly when proceeding into vitellogenesis, stage IV, where all individuals in the subsequent stages had obtained a body weight close to 2 kg (Fig. 7F), indicating body weight as critical for

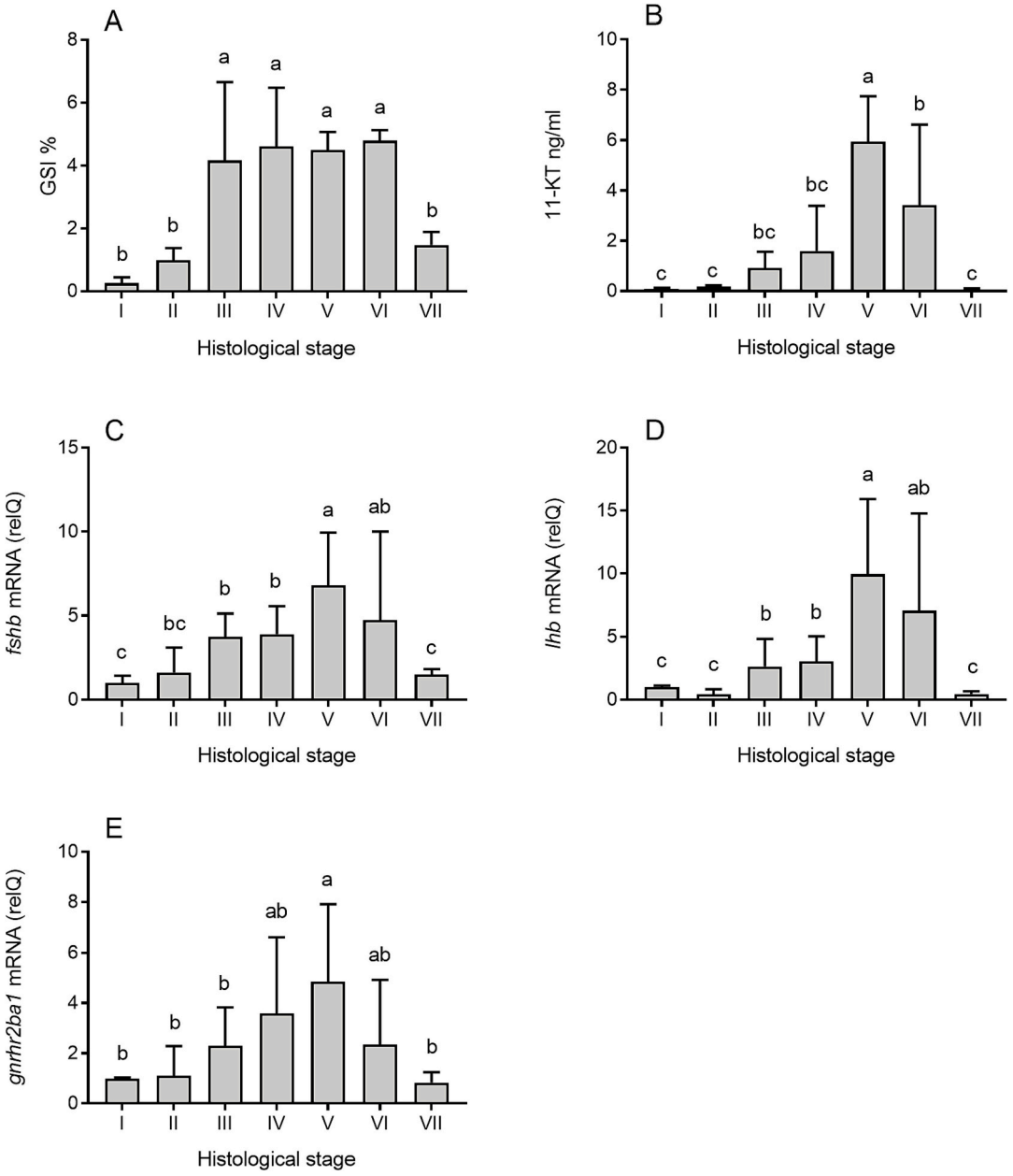

Fig. 8. Comparison of (A) gonadosomatic index (GSI), (B) plasma 11-ketotestosterone (11kT), (C) pituitary *fshb*, (D) *lhb* mRNA levels and (E) *gnrhr2ba1* mRNA levels in lumpfish males at determined stages of testicular development. Data are presented as mean and SD. Shared letters indicates statistical similarities. The number of fish (*N*) was 7 in stage I, 10 in stage II, 14 in stage III, 7 in stage IV, 3 in stage V, 2 in stage VI, 5 in stage VII. Letters indicate significant differences (Student-Newman-Keuls post hoc test, $P < 0.05$) with "a" as the highest value, "b" as the second highest value and "c" as the lowest value.

female lumpfish to continue gametogenesis until spawning. Pountney et al. (2020) also suggested a possible minimum size for recruitment of females into spawning, although lower than our observations. High incidence of atresia in stage I-III females could indicate that even though oocyte development had commenced in those females, their total body energy levels were insufficient to complete maturation. This is, however, speculative and merits further investigation.

Ovarian development and oogenesis in lumpfish followed the same general pattern as in other teleosts (cf Lubzens et al., 2010). Plasma E2 concentrations were highly correlated to stage of development. Our histological and oocyte size frequency analyses showed that lumpfish females have a bimodal oocyte development, and that female lumpfish ready to spawn were restricted to the samplings in February and March as well as in May and June. In February/March, females had stage VII ovaries with two oocyte cohorts maturing with the leading cohort approaching maximum oocyte diameter and by extension very close to becoming ovulated. In May and June, stage VIII ovaries with a single, fully developed cohort of large follicles ready for receiving an ovulatory signal were present. This supports the previous findings by (Gauthier et al., 2017) and (Kennedy, 2018) who suggested that lumpfish females spawn a maximum of two egg batches per season. Pountney et al. (2020) suggested that a proportion of female lumpfish may have a unimodal rather than a bimodal oocyte development. However, in our study the first egg batch was mature in February/March, while the experiment described by Pountney et al., commenced in May, when some females may already have spawned their first batch of eggs.

At the beginning of gametogenesis in male lumpfish, in histological stages I and II, the production of new spermatogenic cysts and their entry into the process of spermatogenesis was observed in both central and peripheral areas of the testis, as evidenced by the presence of

spermatogenic cysts with type A and type B spermatogonia and the increases in testis weight/GSI in these stages. Starting with stage III, however, type B spermatogonia became increasingly rare in central area of the testis and only quiescent, single type A spermatogonia were present, suggesting that cyst production had started to cease in the center. Already existing cysts, on the other hand, continued their development. Since the germ cell number per cyst does no longer increase after completion of meiosis, while germ cells loose mass during spermiogenesis (Schulz et al., 2010; Schulz and Chauvigné, 2018), one can expect a reduction in testis weight. This indeed was recorded in species with a more uniform development of spermatogenesis throughout the testis, such as in different salmonid species (trout [Gomez et al., 1999] Pacific [Campbell et al., 2003] and Atlantic salmon [Melo et al., 2014]). In lumpfish, however, the GSI reached a high level in stage III and remained on that level high up until the spawning season (stage V/VI). We assume that the ongoing cyst production in the periphery of the testicular lobes in stages III and IV not only further increased the size of the testicular lobes via appositional growth, but also prevented the decrease of testis weight usually associated with the loss of cellular mass during spermiogenesis. Finally, we take the decrease of GSI in stage VII as reflecting a combination of the use of spermatozoa during the spawning season and the phagocytosis of residual spermatozoa after the completion of spawning by Sertoli cells. The recycling of valuable building blocks through phagocytosis of spermatozoa reduces the metabolic investment into reproduction for males, and therefore is an important Sertoli cell function.

Typical androgen functions relevant for fish reproduction are, for example, regulating spermatogenesis, reproductive behavior, or the development of secondary sexual characteristics. There is some information on reproductive/spawning behavior of lumpfish (Goulet and Green, 1988; Imsland et al., 2018, 2019; Powell et al., 2018) reporting that the lumpfish spawn in pairs and the males exhibit parental care of the offspring, including territorial/aggressive behavior. The impressive, maturation-associated changes in skin color may indicate that behavioral traits may play a role in context with visual cues communicated by secondary sexual characteristics (Fig. S7). Regarding the latter, it seems that the change in skin color from grey/green to orange/red reflects endogenous androgen bioactivity (Borg, 1982) and can serve as intrinsic bio-indicator for increasing androgen levels (Fig. S7). However, the precipitous decline in plasma 11-KT levels from stage VI to VII is not reflected in a similarly quick change of skin color. This suggests that removal/recycling of pigments, potentially involving biologically precious material (e.g. carotenoids), has a lag time after the decrease of androgen plasma levels. Considering the reproductive development of females, it is interesting to note that intensely colored stage V males with maximum androgen levels were restricted to the samplings in March and May. In the same months, females showed either stage VII or stage VIII ovaries with one oocyte cohort of fully developed, periovulatory follicles.

Regarding the role of androgens on spermatogenesis, the situation in fish is less clear than in mammals. In the latter, androgens are strictly required for the completion of meiosis or spermiogenesis (e.g. De Gendt and Verhoeven, 2012), i.e. androgen insufficiency is incompatible with sperm production in mammals. Also in fish, androgen treatment in vivo (Goos et al., 1986) or androgen exposure of immature testis tissue explants in primary culture promoted germ cell development and induced all stages of spermatogenesis (Miura et al., 1991). However, genetic experiments in medaka (Sato et al., 2008) and zebrafish (Zhai et al., 2018) showed that complete spermatogenesis can also proceed in the presence of very low androgen levels. Furthermore, natural spermatogenesis in three-spined stickleback takes place when androgen plasma levels show their lowest seasonal levels (Hellqvist et al., 2006), while high androgen levels are required for nest-building as well as territorial and courtship behavior, but not for spermatogenesis (see Borg, 1982 for review). In fact, a decrease of androgen levels was required to allow for the start of the next wave of spermatogenic activity (Andersson et al., 1988). This suggests that in fish, spermatogenesis can proceed well even in the presence of low androgen levels. This is the situation we recorded in lumpfish, where the bulk of testis growth was realized when circulating 11-KT levels (stages I – IV), Leydig cell morphology and body coloration suggested basal or limited androgen production. It appears that in fish, in addition to androgens and different from the situation in mammals, a range of other signaling systems can also promote spermatogenesis, such as the Fsh-regulated release of growth factors from Leydig and Sertoli cells, or the also Fsh-responsive production of other small signaling molecules, like retinoic acid and prostaglandins (Crespo et al., 2019), or progesterone (Zhai et al., 2022). Taken together, we assume that the low plasma levels of 11-KT present up until stage IV are sufficient to support spermatogenesis, probably in concert with other, Fsh-regulated signaling systems operating in the growing testis. Indeed, the high 11-KT production attained in the context of preparing the spawning season may end the production of spermatogenic cysts, perhaps by a negative feedback effect on pituitary gonadotropin release, and the resulting reduction of testicular growth factor production.

4.2. *Molecular changes in the pituitary correlated with the histological and physiological changes*

4.2.1. *Gonadotropins*

In female lumpfish, the large individual variation in pituitary *fshb* transcript levels during maturation most likely reflects the bimodal oocyte development with different ovarian oocyte sizes present in the ovary at the same time. A similar situation is present in other multiple spawners such as chub mackerel (Nyuji et al., 2012) European hake (Candelma et al., 2017) and European sea bass (Mateos et al., 2002). In female zebrafish, genetic experiments have shown that loss of the Fsh receptor completely blocks follicle development (Zhang et al., 2015). Future experiments may have to analyse how the Fsh receptor (*fshr*) mRNA levels change in follicle cells depending on the developmental stage of the follicle, i.e., using quantitative in situ hybridisation methods for the *fshr* mRNA to identify the Fsh dependent steps in follicle development.

The profile of *fshb* transcript levels found in male lumpfish is similar to that of salmon (Melo et al., 2014), Atlantic cod (de Almeida et al., 2011) and Senegalese sole (Cerdà et al., 2008), where *fshb* mRNA was up-regulated at the onset of pubertal testis growth, partially down-regulated with the completion of spermatogenesis and fully down-regulated in post spawning fish. This pattern is different from that of male goldfish, sea bream, blue gourami, Japanese flounder, European sea bass and male Atlantic halibut where the expression of both gonadotropins fluctuate in parallel (reviewed by Weltzien et al., 2003; Yaron et al., 2003, 2001).

Consistent with other teleost species, *lhb* transcript levels in both sexes increased in the more advanced stages of maturation: the periovulatory stages in females and spermiogenesis/spermiation in males, reaching peak values at the time of spawning (for review see Levavi-Sivan et al., 2010).

4.2.2. *Gnrh receptors*

Out of the five *gnrhr* forms present in the lumpfish genome, only *gnrhr2ba1*, *−1ca* and *-1cb* were detected in the pituitary of maturing lumpfish, while *-2ba2* and *-2bb* were not detected at all. Furthermore, *−1ca* and *-1cb* were weakly expressed and not regulated during maturation. Altogether, *gnrhr2ba1* was the only Gnrh receptor both expressed and significantly regulated in the pituitary during maturation, both in males and females. *gnrhr2ba1* has consistently been associated with maturation in other Acantomorphs, including medaka (Okubo et al., 2001, 2003; Hodne et al., 2019), European seabass (Madigou et al., 2000; Moncaut et al., 2005), Atlantic cod (von Krogh et al., 2017), chub mackerel (Lumayno et al., 2017), and Astatotilapia (Chen and Fernald, 2006). Signaling of Gnrh through *gnrhr2ba1* in gonadotrophs may be the main pathway in regulation of maturation also in lumpfish.

In lumpfish females, the increase in *gnrhr2ba1* transcript levels preceded that of *lhb*, and its decrease also preceded *lhb* downregulation. We assume that the potential for an increased GnRH response through *gnrhr2ba1* was used and responsible for increasing Lh production. In medaka, *gnrhr2ba1* is almost exclusively expressed in cells that also express *lhb* (Hodne et al., 2019). In European seabass, *gnrhr2ba1* transcripts were localized in all Lh cells and a limited number of Fsh cells (Madigou et al., 2000). In chub mackerel a correlation between *gnrhr2ba1* and *lhb* expression increase in the pituitary was observed during sexual maturation in both sexes (Lumayno et al., 2017). Further experiments would be necessary to determine whether *gnrhr2ba1* signaling also preferentially stimulates Lh release. Indeed, exposure of medaka pituitary cells to Gnrh1 in culture leads to a direct response in Lh cells, while Fsh cells fire spontaneously or are indirectly stimulated by activated Lh cells (Hodne et al., 2019). Moreover, various in vivo and in vitro treatments with endogenous and synthetic Gnrh1 in immature females induced Lh but not Fsh release (Lumayno et al., 2017).

In lumpfish males, *gnrhr2ba1* upregulation did not precede the first increase in *fshb* and *lhb* transcript levels. This suggests that *gnrhr2ba1* is not involved in regulation of early maturation but might be necessary for later maturation stages such as secondary sexual character development. Interestingly, some studies have shown instances where both Fsh and Lh seem to be regulated by Gnrh signaling through *gnrhr2ba1*. In Atlantic cod, *gnrhr2ba1* was expressed in both *fshb*- and *lhb*-expressing cells (von Krogh et al., 2017). In tilapia *gnrhr2ba1* was present in both types of gonadotrophs and was also upregulated in Fsh cells during male maturation. Interestingly, *gnrhr2ba1* was also upregulated in Prl and Sl cells and downregulated in Msh cells in this species, indicating it might be regulating additional endocrine pathways (Parhar et al., 2005). Further research is needed to determine if male lumpfish Fsh cells express the *gnrhr2ba1* gene and directly respond to signaling through it, or if this Fsh regulation is indirect and the result of a coupling between Lh and Fsh cell activity as observed in medaka (Hodne et al., 2019).

In both female and male lumpfish, the first *gnrhr2ba1* upregulation coincides with the first increase in plasma steroid concentrations. This indicates a positive feedback regulation of sex steroids on Gnrh-mediated release of gonadotropins. Circulating steroids might initiate a feedback loop on Gnrh, which would act on *gnrhr2ba1* expression. In the black porgy (*Acanthopagrus schlegeli*), *gnrhr2ba1* expression has indeed been shown to be regulated by gonadotropin analogs, but also E2 and testosterone treatment, both in vitro and vivo (Lin and Ge, 2009).

5. Conclusion

In this study we categorized gametogenesis as histologically defined successive stages in first time maturing lumpfish of both sexes, thus providing a basis for establishing a chronological profile of key physiological mechanisms that regulate reproduction. Gene transcript levels of pituitary Gnrh receptors and gonadotropin beta subunits together with gonadal growth and plasma steroid concentrations were analyzed and their temporal profiles will provide a basis for further investigations.

Author statement

The data presented here are highly relevant for Aquaculture as the effective use of lumpfish for biological delousing of salmon is very important for commercial aquaculture of Atlantic salmon.

Declaration of Competing Interest

There is no conflict of interest in relation to this study.

Data availability

The authors do not have permission to share data.

Acknowledgements

The skillful technical assistance of Anne Torsvik and Grethe Thorsheim at IMR in Bergen is acknowledged. Financial support was given by the Norwegian Research Council (LUSINFER 256199, STAMINA 269043, RFFNord project 282460), Lerøy Seafood Group and the Icelandic Research Council (Rannís, 186971-0611). Opinions expressed and conclusions arrived at, are those of the authors and are not necessarily to be attributed to the funding bodies.

Appendix A. Supplementary data

Supplementary data to this article can be found online at https://doi.org/10.1016/j.aquaculture.2022.739162.

References

Andersen, C.L., Jensen, J.L., Ørntoft, T.F., 2004. Normalization of real-time quantitative reverse transcription-PCR data: a model-based variance estimation approach to identify genes suited for normalization, applied to bladder and colon cancer data sets. Cancer Res. 64, 5245–5250.

Andersson, E., Mayer, I., Borg, B., 1988. Inhibitory effect of 11-ketoandrostenedione and androstenedione on spermatogenesis in the three-spined stickleback, *Gasterosteus aculeatus* L. J. Fish Biol. 33, 835–840.

Bañón, R., Garazo, A., Fernández, A., 2008. Note about the presence of the lumpsucker *Cyclopterus lumpus* (Teleostei, Cyclopteridae) in Galician waters (NW Spain). J. Appl. Ichthyol. 24, 108–1.

Borg, B., 1982. Seasonal effects of photoperiod and temperature on spermatogenesis and male secondary sexual characters in the three-spined stickleback *(Gasterosteus* aculeatus L.). Can. J. Zool. 60, 3377–3386.

Boxaspen, K., 2006. A review of the biology and genetics of sea lice. ICES J. Sea Res. 63, 1304–1316.

Bromage, N., Porter, M., Randall, C., 2001. The environmental regulation of maturation in farmed finfish with special reference to the role of photoperiod and melatonin. Aquaculture 197, 63–98.

Brown-Peterson, N.J., Wyanski, D.M., Saborido-Rey, F., Macewicz, B.J., Lowerre-Barbieri, S.K., 2011. A standardized terminology for describing reproductive development in fishes. Mar. Coast. Fish 3, 52–70.

Campbell, B., Dickey, J.T., Swanson, P., 2003. Endocrine changes during onset of puberty in male spring Chinook salmon *Oncorhynchus tshawytscha*. Biol. Reprod. 69, 2109–2117.

Candelma, M., Fontaine, R., Colella, S., Santojanni, A., Weltzien, F.A., Carnevali, O., 2017. Gonadotropin characterization, localization and expression in the European hake (*Merluccius merluccius*). Reprod. 153, 123–132. https://doi.org/10.1530/REP-16-0377.

Cerdà, J., Chauvigne, F., Agulleiro, M.J., Marin, E., Halm, S., Martínez-Rodríguez, G., Prat, F., 2008. Molecular cloning of Senegalese sole (Solea senegalensis) follicle-stimulating hormone and luteinizing hormone subunits and expression pattern during spermatogenesis. Gen. Comp. Endocrinol. 156, 470–481. https://doi.org/10.1016/j.ygcen.2008.02.006.

Chen, C.C., Fernald, R.D., 2006. Distributions of two gonadotropin- releasing hormone receptor types in a cichlid fish suggest functional specialization. J. Comp. Neurol. 495, 314–323.

Ciani, E., Fontaine, R., Maugars, G., Nourizadeh-Lillabadi, R., Andersson, E., Bogerd, J., von Krogh, K., Weltzien, F.A., 2020. Gnrh receptor gnrhr2bbalpha is expressed exclusively in lhb-expressing cells in Atlantic salmon male parr. Gen. Comp. Endocrinol. 285, 113293.

Collins, M.A., 1976. The lumpfish (*Cyclopterus lumpus* L.) in Newfoundland waters. Can. Field. Nat. 90, 64–67.

Crespo, D., Assis, L.H.C., Kant, H.J.G., van de Waard, S., de Safian, D., Lemos, M.S., Bogerd, J., Schulz, R.W., 2019. Endocrine and local signaling interact to regulate spermatogenesis in zebrafish: follicle-stimulating hormone, retinoic acid and androgens. Development 146, 1-16 /dev.178665.

Cuisset, B., Pradelles, P., Kime, D.E., Kuhn, E.R., Babin, P., Davail, S., Lemenn, F., 1994. Enzyme-immunoassay for 11-ketotestosterone using acetylcholinesterase as label - application to the measurement of 11-ketotestosterone in plasma of Siberian sturgeon. Comp. Biochem. Physiol. C 108, 229–241.

Daborn, G.R., Gregory, R.S., 1983. Occurrence, distribution, and feeding habits of juvenile lumpfish, *Cyclopterus lumpus* L in the bay of Fundy. Can. J. Zool. 61, 797–801.

Davenport, J., 1985. Synopsis of Biological Data of the Lumpsucker *Cyclopterus lumpus* (L 1758). FAO Fisheries Synopsis No. 147, 31 pp.

de Almeida, F.F., Andersson, E., Mittelholzer, C., Karlsen, O., Taranger, G.L., Schulz, R. W., 2011. Pituitary gonadotropin and testicular gonadotropin receptor expression in Atlantic cod (*Gadus morhua* L.) during the first reproductive season: effects of photoperiod modulation. Gen. Comp. Endocrinol. 173, 111–119. https://doi.org/10.1016/j.ygcen.2011.05.002.

De Gendt, K., Verhoeven, G., 2012. Tissue-specific and cell-specific functions of the androgen receptor revealed through conditional knockout models in mice. Mol. Cell. Endocrinol. 352, 13–25.

Denholm, I., Devine, G.J., Horsberg, T.E., Sevatdal, S., Fallang, A., Nolan, D.V., Powell, R., 2002. Analysis and management of resistance to chemotherapeutants in

salmon lice *Lepeophtheirus salmonis* (Krøyer) (Copepoda: Caligidae). Pest Manag. Sci. 58, 528–536.
Fontaine, R., Royan, M.R., von Krogh, K., Weltzien, F.A., Baker, D.M., 2020. Direct and indirect effects of sex steroids on gonadotrope cell plasticity in the teleost fish pituitary. Front. Endocrinol. 11 https://doi.org/10.3389/fendo.2020.605068, 605068.
Gauthier, J., Grégoire, F., Nozères, C., 2017. Assessment of Lumpfish (*Cyclopterus lumpus*) in the Gulf of St. Lawrence (3Pn, 4RS) in 2015. DFO Can. Sci. Advis. Sec. Res. Doc. 2017/051. v + 47 p.
Gomez, J.M., Weil, C., Ollitrault, M., Le Bail, P.Y., Breton, B., Le Gac, F., 1999. Growth hormone (GH) and gonadotropin subunit gene expression and pituitary and plasma changes during spermatogenesis and oogenesis in rainbow trout (*Oncorhynchus mykiss*). Gen. Comp. Endocrinol. 113, 413–428. https://doi.org/10.1006/gcen.1998.7222.
Goos, H.J., de Leeuw, R., van Oordt, P.G., 1986. Gonadotropic hormone-releasing hormone (GnRH) bioactivity in the brain of the immature rainbow trout, Salmo gairdneri: the effect of testosterone. Gen. Comp. Endocrinol. 64, 80–84. https://doi.org/10.1016/0016-6480(86)90031-6 (PMID: 3549432).
Goulet, D., Green, J.M., 1988. Reproductive success of the male lumpfish (*Cyclopterus lumpus* L.) (Pisces: Cyclopteridae): evidence against female mate choice. Can. J. Zool. 66, 2513–2519.
Hellqvist, A., Schmitz, M., Mayer, I., Borg, B., 2006 Feb. Seasonal changes in expression of LH-beta and FSH-beta in male and female three-spined stickleback, *Gasterosteus aculeatus*. Gen. Comp. Endocrinol. 145 (3), 263–269. https://doi.org/10.1016/j.ygcen.2005.09.012. Epub 2005 Nov 11. PMID: 16289183.
Hodne, K., Haug, T.M., Weltzien, F.-A., 2010. Single-cell qPCR on dispersed primary pituitary cells -an optimized protocol. BMC Mol. Biol. 12 (11), 82.
Hodne, K., Fontaine, R., Ager-Wick, E., Weltzien, F.A., 2019. Gnrh1-induced responses are indirect in female medaka fsh cells, generated through cellular networks. Endocrinology 160, 3018–3032.
Imsland, A.K., Reynolds, P., Eliassen, G., Hangstad, T.A., Foss, A., Vikingstad, E., Elvegård, T.A., 2014a. The use of lumpfish (*Cyclopterus lumpus* L.) to control sea lice (*Lepeophtheirus salmonis* Krøyer) infestations in intensively farmed Atlantic salmon (*Salmo salar* L.). Aquaculture 425-426, 18–23.
Imsland, A.K., Reynolds, P., Eliassen, G., Hangstad, T.A., Nytrø, A.V., Foss, A., Vikingstad, E., Elvegård, T.A., 2014b. Assessment of growth and sea lice infection levels in Atlantic salmon stocked in small-scale cages with lumpfish. Aquaculture 433, 137–142.
Imsland, A.K., Reynolds, P., Eliassen, G., Hangstad, T.A., Nytrø, A.V., Foss, A., Vikingstad, E., Elvegård, T.A., 2014c. Notes on behaviour of lumpfish in sea pens with and without Atlantic salmon. J. Ethol. 32, 117–122.
Imsland, A.K., Jonassen, T.M., Hangstad, T.A., Stefansson, S.O., Elvegård, T.A., Lemmens, S.C.A., Urskog, T.C., Nytrø, A.V., Reynolds, P., 2018. The effect of continuous light and compressed photoperiods on growth and maturation in lumpfish *Cyclopterus lumpus*. Aquaculture 485, 166–172.
Imsland, A.K.D., Hangstad, T.A., Jonassen, T.M., Stefansson, S.O., Nilsen, T.O., Hovgaard, P., Elvegård, Lindberg, Mikalsen, B., Urskog, T.C., Norberg, B., Andersson, E., Spetland, F., Reynolds, P., 2019. The use of photoperiods to provide year round spawning in lumpfish *Cyclopterus lumpus*. Comp. Biochem. Physiol. A Bioch 228, 62–70.
Jónsdóttir, Ó.D.B., Schregel, J., Hagen, S.B., Tobiassen, C., Aarnes, S.G., Imsland, A.K.D., 2018. Population genetic structure of lumpfish along the Norwegian coast: aquaculture implications. Aquac. Int. 26, 49–60.
Kennedy, J., 2018. Oocyte size distribution reveals ovary development strategy, number and relative size of egg batches in lumpfish (*Cyclopterus lumpus*). Polar Biol. 41, 1091–1103.
Kennedy, J., Olafsson, H.G., 2019. Conservation of spawning time between years in lumpfish *Cyclopterus lumpus* and potential impacts from the temporal distribution of fishing effort. Fish. Manag. Ecol. 26, 389–396.
Kennedy, J., Jonsson, S.P., Kasper, J.M., Olafsson, H.G., 2015. Movements of female lumpfish (*Cyclopterus lumpus*) around Iceland. ICES J. Mar. Sci. 72, 880–889.
Levavi-Sivan, B., Bogerd, J., Mañanós, E.L., Gómez, A., Lareyre, J.J., 2010. Perspectives on fish gonadotropins and their receptors. Gen. Comp. Endocrinol. 165, 412–437.
Lin, S.-W., Ge, W., 2009. Differential regulation of gonadotropins (FSH and LH) and growth hormone (GH) by neuroendocrine, endocrine, and paracrine factors in the zebrafish – an in vitro approach. Gen. Comp. Endocrinol. 160, 183–193.
Lorgen, M., Casadei, E., Król, E., Douglas, A., Birnie, M.J., Ebbesson, L.O., Nilsen, T.O., Jordan, W.C., Jørgensen, E.H., Dardente, H., Hazlerigg, D.G., Martin, S.A., 2015. Functional divergence of type 2 deiodinase paralogs in the Atlantic salmon. Curr. Biol. 25, 936–941.
Lubzens, E., Young, G., Bobe, J., 2010. Oogenesis in teleosts: how eggs are formed. Gen. Comp. Endocrinol. 165, 367–389.
Lumayno, S.D.P., Ohga, H., Selvaraj, S., Nyuji, M., Yamaguchi, A., Matsuyama, M., 2017. Molecular characterization and functional analysis of pituitary GnRH receptor in a commercial scombroid fish, chub mackerel (Scomber japonicus). Gen. Comp. Endocrinol. 247, 143–151.
Madigou, T., Mananos-Sanchez, E., Hulshof, S., Anglade, I., Zanuy, S., Kah, O., 2000. Cloning, tissue distribution, and central expression of the gonadotropin-releasing hormone receptor in the rainbow trout (*Oncorhynchus mykiss*). Biol. Reprod. 63, 1857–1866.
Mateos, J., Mañanos, E., Carrillo, M., Zanuy, S., 2002. Regulation of follicle- stimulating hormone (FSH) and luteinizing hormone (LH) gene expression by gonadotropin-releasing hormone (GnRH) and sexual steroids in the mediterranean sea bass. Comp. Biochem. Physiol. 132B, 75–86.
Melo, M.C., Andersson, E., Fjelldal, P.G., Bogerd, J., Franca, L.R., Taranger, G.L., Schulz, R.W., 2014. Salinity and photoperiod modulate pubertal development in Atlantic salmon (*Salmo salar*). J. Endocrinol. 220, 319–332.
Mitamura, H., Thorstad, E.B., Uglem, I., Bjørn, P.A., Okland, F., Naesje, T.F., Dempster, T., Arai, N., 2012. Movements of lumpsucker females in a northern Norwegian fjord during the spawning season. Environ. Biol. Fish 93, 475–481.
Miura, T., Yamauchi, K., Takahashi, H., Nagahama, Y., 1991. Hormonal induction of all stages of spermatogenesis in vitro in the male Japanese eel (*Anguilla japonica*). Proc. Natl. Acad. Sci. 88, 5774–5778. https://doi.org/10.1073/pnas.88.13.5774. PMID: 2062857; PMCID: PMC51960.
Moncaut, N., Somoza, G., Power, D.M., Canario, A.V., 2005. Five gonadotrophin-releasing hormone receptors in a teleost fish: iso- lation, tissue distribution and phylogenetic relationships. J. Mol. Endocrinol. 34, 767–779.
Nguyen, N.T.T., Vincens, P., Roest Crollius, H., Louis, A., 2019. Genomicus 2018: karyotype evolutionary trees and on-the-fly synteny computing. Nuc. Ac. Res. 2017 https://doi.org/10.1093/nar/gkx1003.
Normann, K.R., Øystese, K.A.B., Berg, J.P., Lekva, T., Berg-Johnsen, J., Bollerslev, J., Olarescu, N.C., 2016. Selection and validation of reliable reference genes for RT-qPCR analysis in a large cohort of pituitary adenomas. Mol. Cell. Endocrinol. 437, 183–189.
Norwegian Directorate of Fisheries, 2019. Sale of Farmed Cleaner Fish 2012-2019. Available from URL: https://www.fiskeridir.no/English/Aquaculture/Statistics/Cleanerfish-Lumpfish-and-Wrasse.
Nyuji, M., Selvaraj, S., Kitano, H., Ohga, H., Yoneda, M., Shimizu, A., Kaneko, K., Yamaguchi, A., Matsuyama, M., 2012. Changes in the expression of pituitary gonadotropin subunits during reproductive cycle of multiple spawning female chub mackerel *Scomber japonicus*. Fish Physiol. Biochem. 38, 883–897. https://www.fiskeridir.no/English/Aquaculture/Statistics/Cleanerfish-Lumpfish-and-Wrasse.
Okubo, K., Nagata, S., Ko, R., Kataoka, H., Yoshiura, Y., Mitani, H., Kondo, M., Naruse, K., Shima, A., Aida, K., 2001. Identification and characterization of two distinct GnRH receptor subtypes in a teleost, the medaka *Oryzias latipes*. Endocrinol. 142, 4729–4739.
Okubo, K., Ishii, S., Ishida, J., Mitani, H., Naruse, K., Kondo, M., Shima, A., Tanaka, M., Asakawa, S., Shimizu, N., Aida, K., 2003. A novel third gonadotropin- releasing hormone receptor in the medaka *Oryzias latipes*: evolutionary and functional implications. Gene 314, 121–131.
Pampoulie, C., Skírnisdottir, S., Ólafsdóttir, G., Helyar, S.J., Thorsteinsson, V., Jónsson, S.Þ., Fréchet, A., Durif, C.M.F., Sherman, S., Lampart-Kałużniacka, M., Hedeholm, R., Ólafsson, H., Daníelsdóttir, A.K., Kasper, J.M., 2014. Genetic structure of the lumpfish *Cyclopterus lumpus* across the North Atlantic. ICES J. Mar. Sci. 71, 2390–2397.
Pankhurst, N.W., Carragher, J.F., 1992. Oocyte maturation and changes in plasma steroid-levels in snapper *Pagrus (chrysophrys) auratus* (Sparidae) following treatment with human chorionic-gonadotropin. Aquaculture 101, 337–347.
Parhar, I.S., Ogawa, S., Sakuma, Y., 2005. Three GnRH receptor types in laser-captured single cells of the cichlid pituitary display cellular and functional heterogeneity. Proc. Natl. Acad. Sci. U. S. A. 102, 2204–2209.
Paullada-Salmerón, J.A., Cowan, M., Aliaga-Guerrero, M., López-Olmeda, J.F., Mañanós, E.L., Zanuy, S., Muñoz-Cuet, J.A., 2016. Testicular steroidogenesis and locomotor activity are regulated by gonadotropin-inhibitory hormone in male European sea bass. PLoS One 11, e0165494.
Pfaffl, M.W., Tichopad, A., Prgomet, C., Neuvians, T.P., 2004. Determination of stable housekeeping genes, differentially regulated target genes and sample integrity: BestKeeper–Excel-based tool using pair-wise correlations. Biotechnol. Lett. 26, 509–515.
Pountney, S.M., Lein, I., Migaud, H., Davie, A., 2020. High temperature is detrimental to captive lumpfish (Cyclopterus lumpus, L) reproductive performance. Aquaculture 522, 735121.
Powell, A., Treasurer, J.W., Pooley, C.L., Keay, A.J., Lloyd, R., Imsland, A.K., Garcia de Leaniz, C., 2018. Use of lumpfish for sea-lice control in salmon farming: challenges and opportunities. Rev. Aquac. 10, 683–702.
Sato, T., Suzuki, A., Shibata, N., Sakaizumi, M., Hamaguchi, S., 2008 Mar. The novel mutant scl of the medaka fish, Oryzias latipes, shows no secondary sex characters. Zool. Sci. 25 (3), 299–306. https://doi.org/10.2108/zsj.25.299 (PMID: 18393567).
Schulz, R.W., Chauvigné, F., 2018. Spermatogenesis and spermiogenesis, fish. In: Skinner, M.K. (Ed.), Encyclopedia of Reproduction, , 2nd editionvol. 6. Academic Press, Elsevier, pp. 297–304.
Schulz, R.W., de França, L.R., Lareyre, J.J., Le Gac, F., Chiarini-Garcia, H., Nobrega, R.H., Miura, T., 2010. Spermatogenesis in fish. Gen. Comp. Endocrinol. Comp. Endocrinol. 165, 390–411.
Sefideh, F.A., Moon, M.J., Yun, S., Hong, S.I., Hwang, J.-I., Seong, J.Y., 2014. Local duplication of gonadotropin-releasing hormone (GnRH) receptor before two rounds of whole genome duplication and origin of the mammalian GnRH receptor. PLoS One 9, e87901.
Silver, N., Best, S., Jiang, J., Thein, S.L., 2006. Selection of housekeeping genes for gene expression studies in human reticulocytes using real-time PCR. BMC Mol. Biol. 7, 33.
Singh, P.P., Isambert, H., 2019. OHNOLOGS v2: a comprehensive resource for the genes retained from whole genome duplication in vertebrates. Nucl. Ac. Res. 48, D724–D730.
Taranger, G.L., Carrillo, M., Schulz, R.W., Fontaine, P., Sanuy, S., Felip, A., Weltzien, F. A., Dufour, S., Karlsen, Ø., Norberg, B., Andersson, E., Hansen, T., 2010. Control of puberty in farmed fish. Gen. Comp. Endocrinol. 165, 483–515.
Thorsen, A., Kjesbu, O.S., 2001. A rapid method for estimation of oocyte size and potential fecundity in Atlantic cod using a computer-aided particle analysis system. J. Sea Res. 46, 295–308.

Treasurer, J.W., 2018. An introduction to sea lice and the rise of cleaner fish. Cleaner fish biology and aquaculture applications. In: Treasurer, J.W. (Ed.), Cleaner Fish Biology and Aquaculture Applications. 5M Publishing Ltd., Sheffield, pp. 3–24.

Trudeau, 2022. Neuroendocrine control of reproduction in Teleost fish: Concepts and controversies. Annu. Rev. Anim. Biosci. 10, 107–130.

Vandesompele, J., De Preter, K., Pattyn, F., Poppe, B., Van Roy, N., De Paepe, A., Speleman, F., 2002. Accurate normalization of real-time quantitative RT-PCR data by geometric averaging of multiple internal control genes. Genome Biol. 23. RESEARCH0034.

Vasconcelos, P., Monteiro, C.C., Santos, M.N., Gaspar, B., 2004. First record of the lumpfish (*Cyclopterus lumpus* Linnaeus, 1758) off the Algarve coast (southern Portugal): southward extension of the species distributional range. J. Appl. Ichthyol. 20, 159–160.

von Krogh, K., Bjørndal, G.T., Nourizadeh-Lillabadi, R., Hodne, K., Ropstad, E., Haug, T. M., Weltzien, F.-A., 2017. Sex steroids differentially regulate fshb, lhb and gnrhr expression in Atlantic cod (*Gadus morhua*). Reprod. 154, 581–594.

Wallace, R.A., Selman, K., 1990. Ultrastructural aspects of oogenesis and oocyte growth in fish and amphibians. J. Electron Microsc. Tech. 16, 175–201.

Wang, L., Burger, L.L., Greenwald-Yarnell, M.L., Myers Jr., M.G., Moenter, S.M., 2018. Glutamatergic transmission to hypothalamic kisspeptin neurons is differentially regulated by estradiol through estrogen receptor α in adult female mice. J. Neurosci. 38, 1061–1072.

Weltzien, F.-A., Kobayashi, T., Andersson, E., Norberg, B., Andersen, Ø., 2003. Molecular characterization and expression of FSHβ, LHβ, and the α-subunit in male Atlantic halibut (*Hippoglossus hippoglossus* L.). Gen. Comp. Endocrinol. 131, 87–96.

Xie, F., Xiao, P., Chen, D., Xu, L., Zhang, B., 2012. miRDeepFinder: a miRNA analysis tool for deep sequencing of plant small RNAs. Plant Mol. Biol. https://doi.org/10.1007/s11103-012-9885-2.

Yaron, Z., Gur, G., Melamed, P., Rosenfeld, H., Levavi-Sivan, B., Elizur, A., 2001. Regulation of gonadotropin subunit genes in tilapia. Comp. Biochem. Physiol. B Biochem. Mol. Biol. 129, 489–502.

Yaron, Z., Gur, G., Melamed, P., Rosenfeld, H., Elizur, A., Levavi-Sivan, B., 2003. Regulation of fish gonadotropins. Int. Rev. Cytol. 225, 131–185.

Zhai, G., Shu, T., Xia, Y., Lu, Y., Shang, G., Jin, X., He, J., Nie, P., Yin, Z., 2018 Oct 1. 2018. Characterization of sexual trait development in cyp17a1-deficient zebrafish. Endocrinol. 159 (10), 3549–3562. https://doi.org/10.1210/en.2018-00551. 30202919.

Zhai, G., Shu, T., Yu, G., Tang, H., Shi, C., Jia, J., Lou, Q., Dai, X., Jin, X., He, J., Xiao, W., Liu, X., Yin, Z., 2022 Feb 28. 2022. Augmentation of progestin signaling rescues testis organization and spermatogenesis in zebrafish with the depletion of androgen signaling. Elife 11. https://doi.org/10.7554/eLife.66118 e66118. PMID: 35225789; PMCID: PMC8912926.

Zhang, Z., Lau, S.W., Zhang, L., Ge, W., 2015 Oct. 2015. Disruption of zebrafish follicle-stimulating hormone receptor (fshr) but not luteinizing hormone receptor (lhcgr) gene by TALEN leads to failed follicle activation in females followed by sexual reversal to males. Endocrinology. 156 (10), 3747–3762. https://doi.org/10.1210/en.2015-1039. Epub 2015 May 20. 25993524.

Zinzow-Kramer, W.M., Horton, B.M., Maney, D.L., 2014. Evaluation of reference genes for quantitative real-time PCR in the brain, pituitary, and gonads of songbirds. Horm. Behav. 66, 267-75.